Tetrahedron 66 (2010) 2520–2528

Contents lists available at ScienceDirect

Tetrahedron

journal homepage: www.elsevier.com/locate/tet

Synthesis of new mono and bis amides projected as potential histone deacetylase (HDAC) inhibitors

Stefania Terracciano, Maria Giovanna Chini, Giuseppe Bifulco, Elisabetta D'Amico, Stefania Marzocco, Raffaele Riccio, Ines Bruno *

Dipartimento di Scienze Farmaceutiche, Università degli Studi di Salerno, Via Ponte Don Melillo, 84084 Fisciano (SA), Italy

ARTICLE INFO

Article history:
Received 18 May 2009
Received in revised form 9 December 2009
Accepted 18 January 2010
Available online 22 January 2010

Keywords:
Histone deacetylase
Ring closing metathesis reaction
Anticancer drugs
Docking studies

ABSTRACT

In our ongoing efforts to discover new potent histone deacetylase (HDAC) inhibitors as promising anticancer candidates, we designed and synthesized a small collection of 3-substituted amines possessing macro heterocyclic skeletons bearing variable-length tails. As a metal binder domain, all the compounds possess an amide function suitable for Zn^{2+} chelation in the enzyme active site. A combination of solution and solid phase techniques were employed to synthesize the compounds and, as the key synthetic step to obtain the rings, a ring closing metathesis (RCM) reaction was adopted. The putative affinity of the compounds for the histone deacetylase-like protein (HDLP) model receptor active site was explored through docking calculations, and we also report preliminary studies on their pharmacological properties.

1. Introduction

The epigenetic modulators[1] have emerged as new and attractive therapeutics as a consequence of their ability to influence transcriptional events. Histone deacetylases (HDACs), in fact, have been recently highlighted as promising targets in the epigenetic therapy for the treatment of several disorders including cancer, as they are responsible, together with histone acetyl transferase (HAT), for the acetylation level of histone proteins which, in turn, is associated to the transcriptional state of chromatin.[2] The great potential of HDAC inhibitors as anticancer drugs seems to be related to the transcription and expression of oncogenes, which are silent in cancer pathology. In the course of our research on bioactive natural products as useful tools in the drug discovery field, we recently focused our interest on FR235222,[3] a natural cyclopeptide possessing a potent HDAC inhibitory activity and whose total synthesis has been successfully realized by us.[4] With the aim of gaining more information on the nature of the interaction between this structural class of inhibitors and the biological target, a first collection of FR235222 cyclopeptidic analogues was efficiently synthesized[5] and their biological profile was also evaluated in order to identify some structural aspects involved in the activity modulation. At the same time, through molecular docking calculations, a 3D model of the interaction between a potential ligand and the active site of HDPL,[6] the bacterial homologue of human HDAC, was also proposed, in order to clarify the influence of some structural elements exploitable for a further structural optimization process.[7] Basing on the advances made in receptor mapping knowledge, we decided to explore the effect on HDAC of entirely non-peptidic compounds, having, as the binding recognition domain, macro-heterocycles or substituted amines, and possessing, as metal binders, amide functions, which proved to be very efficient in the case of the azumamides,[8] to produce the crucial Zn chelation event. Here, we report the design, virtual screening, and synthesis of this new collection of compounds, whose cytotoxic properties are also described.

2. Results and discussion

The present work can be considered a further evolution of our ongoing project involved in the discovery of new potential HDAC inhibitors; in this regard, having only experience with compounds

Abbreviations: 4-aba, 4-allyloxybenzaldehyde; 4-Pea, 4-pentenoic acid; 6-Epa, 6-eptenoic acid; BAP, borane–pyridine complex; Boc, *tert*-butyloxycarbonyl; DCM, dichloromethane; DIC, *N*,*N*′, diisopropyl-carbodiimide; DIEA, *N*,*N*-diisopropylethylamine; DMF, *N*,*N*-dimethylformamide; Fmoc, 9-fluorenylmethyloxycarbonyl; Fmoc-6-Ahx-OH, Fmoc-6-aminohexanoic acid; Fmoc-8-Aoc-OH, Fmoc-8-aminooctanoic acid; Grubbs second gen., Grubbs catalyst second generation; HBTU, *O*-(benzotriazol-1-yl)-1,1,3,3-tetramethyluronium hexafluorophosphate; HOBt, *N*-hydroxybenzotriazole; NMM, *N*-methylmorpholine; Rink Amide MBHA resin, 4-(2′,4′-dimethoxyphenyl-Fmoc-aminomethyl)-phenoxyacetamico-norleucyl-MBHA resin; RCM, ring closing metathesis; TFA, trifluoroacetic acid; TFE, 2,2,2-trifluoroethanol; TIS, triisopropylsilane; TMOF, trimethyl orthoformate; TNBS, 2,4,6-trinitrobenzenesulfonic acid; Uda, undecylenic aldehyde.

* Corresponding author. Tel.: +39 089 969743; fax: +39 089 969702.
E-mail address: brunoin@unisa.it (I. Bruno).

0040-4020/$ – see front matter © 2010 Elsevier Ltd. All rights reserved.
doi:10.1016/j.tet.2010.01.061

of a cyclopeptide nature and aimed at further increasing the in vivo stability of the potential HDAC binders, we decided to reproduce, to some extent, the molecular shape of our previous synthetic compounds,[5] but, instead of the cyclopeptide framework, we utilized heterocyclic moieties or open chain tertiary amines, bearing a terminal functionalized aliphatic chain of appropriate length. As the metal binder domain, we selected the amide functionality present in other potent HDAC inhibitors of natural origin, such as the azumamides.[8] Concerning the retrosynthetic plan of our molecules, we immediately recognized the possibility of applying, the ring closing metathesis (RCM) reaction,[9] as the key step to close the rings, which has emerged as a powerful tool for the construction of carbocyclic and heterocyclic ring systems. On the basis of this assumption, and in consideration of the commercial availability of the building blocks, we designed seven molecules (Scheme 1), five of which (**1**, **2**, **3**, **6**, **7**) possessing, as cap group, cyclic structures of different size, and bearing variable-length functional tails; the other two (**4**, **5**) mainly represent, to some extent, the open versions of the previous ones.

The first step was a docking study on the designed molecules to obtain a prediction of their histone deacetylases inhibitory activity, through virtual screening process. Prior to the docking calculations, we performed a conformational search on the cyclic[10] compounds by means of molecular dynamics at different temperatures (400, 600, and 800 K) using the MMFFs[11] force field included in the MacroModel software package.[12] On the so-obtained model, QM optimization of the energies and the geometries was performed in vacuo at the hybrid DFT B3LYP level, using the 6-31G(d) basis set (Gaussian 03 Software Package).[13] Subsequently, the charges of **1**–**7** were calculated with the ChelpG method[14] at the B3LYP/6-31G+(d) level.

Docking studies were performed on compounds **1**–**7** with the HDLP binding pocket,[6] using AutoDock 3.0.5 software,[15] which has been successfully used in the interpretation of the inhibitory activity of several HDAC ligands.[7,16] In addition to the compounds optimized as described above, we used as model receptor the HDLP active site refined at the QM level[17] by us in previous studies,[16d] in order to improve our calculations with the aim to obtain a good qualitative accordance between theoretical K_d and biological assays results. According to the receptor mapping, besides the binding channel (11 Å) there are four hydrophobic cavities (A–D)[16a] acting as the molecular recognition domain (Fig. 1).

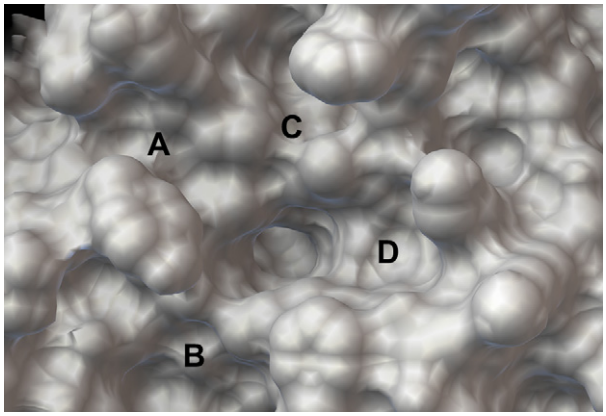

Figure 1. 3D model of the HDLP.

The results obtained (Table 1) showed satisfactory K_d values for all compounds, even if among them, compounds **6** and **7** showed a little better binding properties for the HDLP receptor surface.

Concerning all cyclic molecules (**1**–**3**, **6**, **7**), docking studies suggest strong interactions between the recognition binding domain, represented by the heterocyclic framework, and the hydrophobic surface of the HDLP active site. For the sake of simplicity, we will only describe the detailed docking results for compounds **1** and **7**, the latter showing the best calculated affinity for the target.

Our docking studies indicate that the linker chain and the cap group of **7** and **1** fill equivalent spaces (hydrophobic pocket D: H170, A197, L265, F198, and F200). Moreover, the linker chain exerts a set of interactions with the tubular hydrophobic pocket and the zinc-coordinating amidic group, forming hydrogen bonds with $H^{\varepsilon 2}$ of H131.

The cap group portion of both compounds is accommodated in a shallow groove, establishing Van der Waals interactions and hydrogen bonds with the receptor counterpart, formed by H170, A197, F198, and F200 residues. The cap group extends its hydrophobic contacts thanks to the phenyl ring, which is accommodated in the deep pocket D (Y264, L265, S266, K267, see Fig. 2); however, the macrocycle size seems to slightly modulate the activity, as emerged by directly comparing **1** with **7**; this last compound, in fact, in virtue

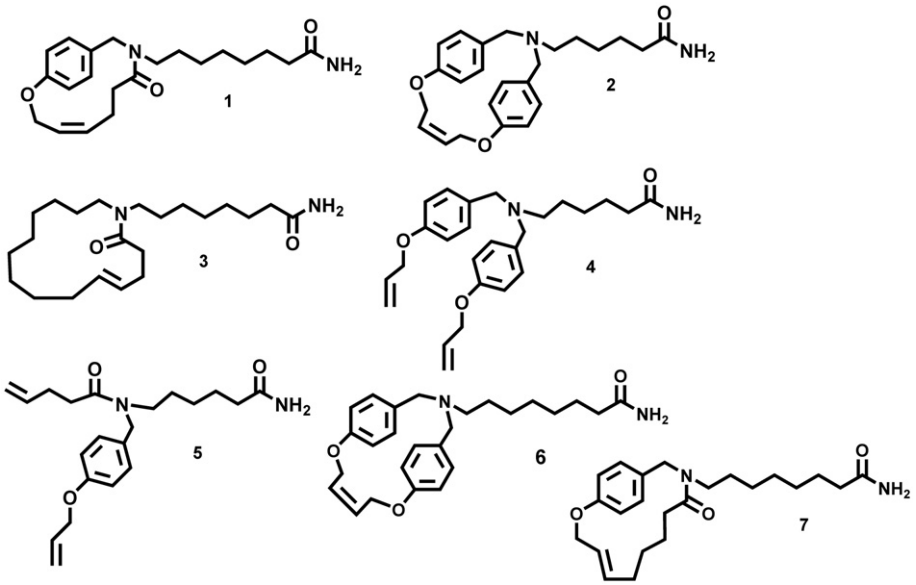

Scheme 1. Molecular structures of **1**–**7** compounds.

Table 1
Calculated (K_d) activities of **1–7** compounds

	1	2	3	4	5	6	7
$K_{d.}$	1.78×10^{-8}	4.09×10^{-8}	7.81×10^{-8}	2.74×10^{-8}	3.65×10^{-7}	8.88×10^{-9}	1.82×10^{-9}

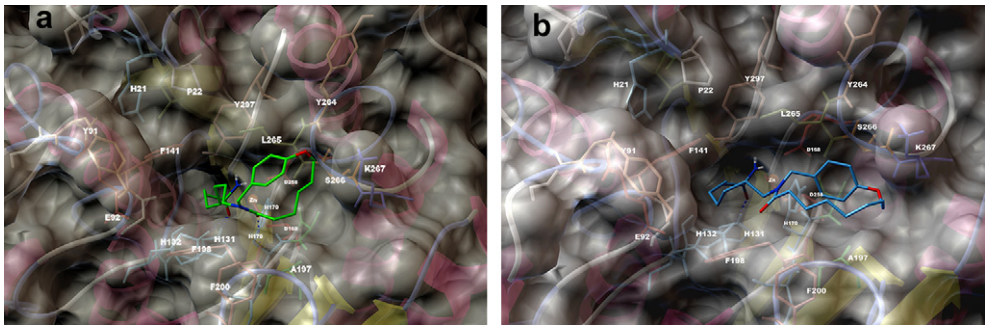

Figure 2. (a) 3D model of the interaction between **1** and the HDLP binding site. The protein is represented by molecular surface and sticks and balls. Compound **1** is depicted by sticks (by atom type: C green, polar H white, N dark blue, O red). (b) 3D model of the interaction between **7** and the HDLP binding site. The protein is represented by molecular surface and sticks and balls. Compound **7** is depicted by sticks (by atom type: C sky blue, polar H white, N dark blue, O red).

of its higher dimension of the cycle (13 C atoms vs 15, respectively) showed to fit better with the enzyme binding domain. In fact, the suboptimal hydrophobic interactions are responsible for a predicted increase in the binding affinity to the receptor of about 10-fold (K_d of **1** 1.78×10^{-8} vs K_d of **7** 1.82×10^{-9}).

Furthermore, comparing the docking results of **2** and **6** (Fig. 3), presenting the same cap group but differing for the linker length, we can suppose that it should be of nine carbon atoms in order to have the optimal fit with receptor surface.

but, at the same time, allowed us to make some considerations on the virtual screening outcome.

For example, the predicted negative response for some of the designed molecules (in good qualitative accordance with the experimental data) can be ascribed to unfavorable structural features, such as the lack of aromatic rings in compound **3**, while, the unsuitable size of the aliphatic chain spacer in **2** could account for the absence of cytotoxicity, in coherence with its slightly less satisfactory K_d value.

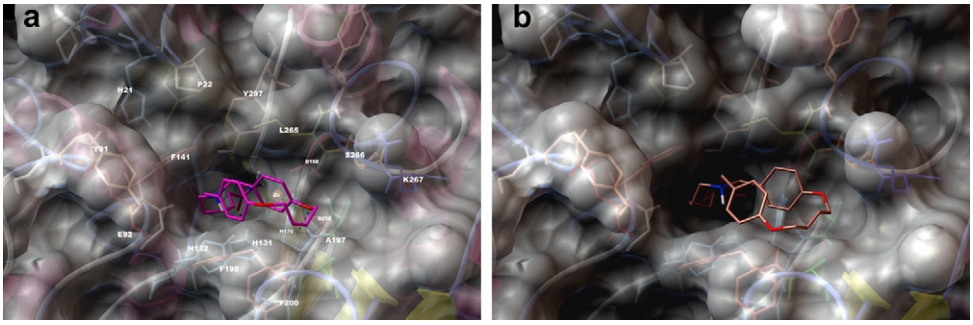

Figure 3. (a) 3D model of the interaction between **2** and the HDLP binding site. The protein is represented by molecular surface and sticks and balls. Compound **2** is depicted by sticks (by atom type: C violet, polar H white, N dark blue, O red). (b) 3D model of the interaction between **6** and the HDLP binding site. The protein is represented by molecular surface and sticks and balls. Compound **6** is depicted by sticks (by atom type: C pink, polar H white, N dark blue, O red).

Finally, compound **3**, which presents the same linker as **6**, but an entirely aliphatic cap group (Fig. 4), could not establish strong hydrophobic interactions with the protein counterpart, being totally lacking of aromatic elements with respect to the other cyclic compounds.

For the analysis of linear compounds **4** and **5**, the small difference of their K_d values, could be ascribed to their different aromatic ring content. In fact, the two aromatic rings present in compound **4** were correctly accommodated in the A and D hydrophobic pockets (see Supplementary data) of the enzyme, increasing the stability of the drug–receptor complex (Fig. 5).

Prompted by the virtual screening results, we decided to undertake the synthesis of the designed molecules aimed at verifying the qualitative accordance between the theoretical and the experimental data (see Chemistry section). A cytotoxicity assay was then performed on the synthesized molecules and the analysis of the results, reported in Table 2, was disappointing for some compounds

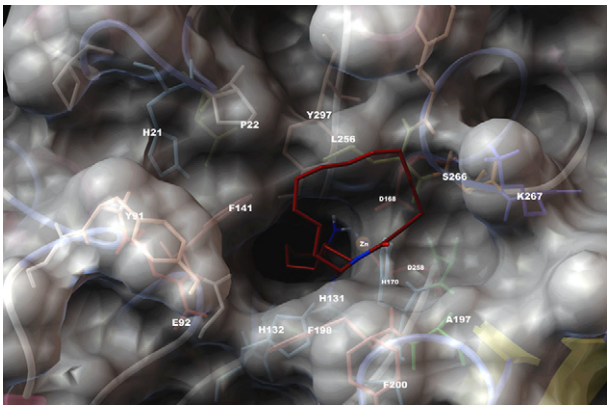

Figure 4. 3D model of the interaction between **3** and the HDLP binding site. The protein is represented by molecular surface and sticks and balls. Compound **3** is depicted by sticks (by atom type: C dark red, polar H white, N dark blue, O red).

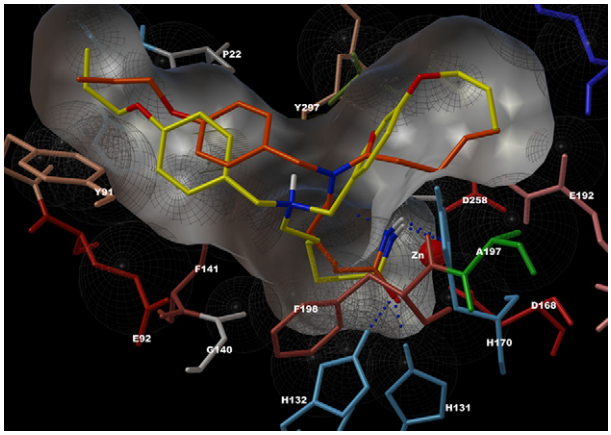

Figure 5. Compounds **4** and **5** superimposition in the zinc-binding site.

was performed through a ring closing metathesis (RCM) reaction, which represents a suitable approach for the construction of variable-sized macrocyclic ring systems.[22] As suggested by our previous studies we used second-generation Grubbs' catalyst, which was found to be more stable and more reactive in our reaction conditions. RCM reactions were carried out using microwave irradiation, which enhanced the reaction rate. The optimal conditions found were: 0.3 mM solutions, 10 mol % of Grubbs catalyst second generation, DCM as solvent and microwave heating at 300 W for two 40 min periods. The structures of the desired compounds were confirmed by mass spectrometry and analytical RP-HPLC. The crude products were purified by semipreparative RP-HPLC on a C18 column and the structures of **1**–**3** and **6**, **7** (20–33% yield after two purification HPLC steps) were confirmed by MS and NMR spectroscopic analysis. The ^{1}H and ^{13}C NMR spectra showed that the RCM reactions lead only to the *Z*-olefin-stereoisomer for compounds **2** and **6**, while compounds **1**, **3**, and **7** were obtained as a mixture of cis and trans isomers. [23] Unfortunately, we were unable to separate the isomers by semipreparative HPLC.

Table 2
Biological (IC_{50}) activities of compounds **1**–**7** on HEK-293, J774A.1, and WEHI-164. Control cells viability was designated as 100%, and results were expressed as the concentration of tested compounds able to induce the 50% of mortality in cells (IC_{50}). Results are expressed as mean±SEM from at least three-independent experiments

	1	**2**	**3**	**4**	**5**	**6**	**7**
IC_{50} [M] HEK-293	$1.85\times10^{5}\pm0.04$	n.d.	n.d.	$7.49\times10^{-5}\pm0.72$	n.d.	$1.4\times10^{-5}\pm0.03$	$1.0\times10^{-4}\pm0.02$
IC_{50} [M] WEHI-164	$2.0\times10^{-5}\pm0.05$	$3.0\times10^{-4}\pm0.02$	n.d.	$3.2\times10^{-4}\pm0.21$	n.d.	$2.4\times10^{-5}\pm0.05$	$2.2\times10^{-5}\pm0.08$
IC_{50} [M] J774A.1	$2.4\times10^{-5}\pm0.18$	n.d.	n.d.	$7.38\times10^{-5}\pm0.12$	n.d.	n.d.	$2.4\times10^{-4}\pm0.13$

In contrast, as concerns compounds **6** and **7**, the biological results were in disagreement with the virtual screening response. In fact, these two compounds, despite displaying the best affinity properties in docking studies, did not exert the expected higher potency in antiproliferative assay, probably due to unfavorable pharmacokinetic parameters—such parameters are in fact not quantifiable in the computer simulation approach.

3. Chemistry

The synthesis of compounds **1**–**7** is depicted in Schemes 2 and 3. Attachment of the starting amino acid residue to the previously deprotected Rink Amide MBHA resin was performed with HOBt and DIC in DMF for 3 h, and the obtained loading degree was determined by UV spectrophotometric analysis. After the acetylation step, the Fmoc protecting group was removed by treatment with a 20% solution of piperidine in *N*,*N*-dimethylformamide (DMF). Alkylation of the primary amine with the aldehydes (5 equiv), on solid phase, was performed in a two-step procedure in order to minimize dialkylation[18] reaction and employing $(MeO)_3CH$ (TMOF) as both solvent and dehydrating agent.[19] Reduction of the intermediate imines was achieved by reaction with borane–pyridine complex ($BH_3\cdot Py$, BAP) at room temperature overnight.[20] The reaction was monitored (after a mini-cleavage step from the resin) by HPLC analysis and ESI MS; data obtained indicated clean and high yielding reactions. For the synthesis of compounds **1**, **3**, **5**, and **7** the coupling of the secondary amines with the appropriate carboxylic acids was obtained using HOBt/HBTU, with 5 equiv of reagents, in DIPEA (10 equiv). For the synthesis of the linear precursors of compounds **2**, **4**, and **6**, instead, a second reductive alkylation step of the secondary amine function was realized (Scheme 3).

This was performed using the aldehyde (10 equiv) in TMOF and BAP (10 equiv) at room temperature for 4 days; the dialkylated products were obtained in quantitative yields.[21] The linear precursors were cleaved from the resin, by a single step treatment with a TFA/TIS/H_20 95:2.5:2.5 solution, according to general procedure *e* (81–97% overall yield with greater than 95% purity). Finally, for the synthesis of compounds **1**–**3** and **6**, **7**, the intramolecular cyclization

4. Conclusion

A new collection of potential HDAC inhibitors has been developed and a partial rationalization of their biological behavior has been pursued through Molecular docking calculations. Four of the seven synthesized molecules showed a satisfying level of antiproliferative activity and all of them are currently investigating for their ability to inhibit HDAC enzyme.

5. Experimental section

5.1. Molecular mechanics and dynamics calculations

Molecular mechanics/dynamics (MM and MD) calculations were performed using the Macromodel 8.5 software package[11] and the MMFFs[24] force field at several temperatures (400, 600, and 800 K). The solvent effects are simulated using the analytical Generalized-Born/Surface-Area[25] (GB/SA) model mimicking the presence of H_2O. All the structures were minimized using a Polak-Ribiere Conjugate Gradient (PRCG, 50,000 steps, maximum derivative less than 0.005 kcal/mol).

5.2. Docking studies

Autodock 3.0.5[15] was used for all docking calculations. HDLP [6] (histone deacetylase-like protein) is a metalloprotein, so a nonbonded model for metallic center according to the nonbonded Zn parameters of Stote[26] (Zinc radius=1.10 Å, well depth=0.25 kcal/mol) was used. In order to have an accurate weight of the electrostatics, we derived the partial charge of Zn=1.175 and of the amino acids involved in the catalytic center (A169, H170, D168, D258) by DFT calculations B3LYP level by the 6-31G(d) basis set and ChelpG method [14]for population analysis (Gaussian 03 Software Package).[13] For what concerns the ligands, the geometries were optimized (see Supplementary data) at the hybrid DFT B3LYP level using the 6-31G(d) basis set. Subsequently, the charges of compounds **1**–**7** were calculated with the ChelpG method[14] at the B3LYP/6-31G+(d) level. The above calculated charges were used for

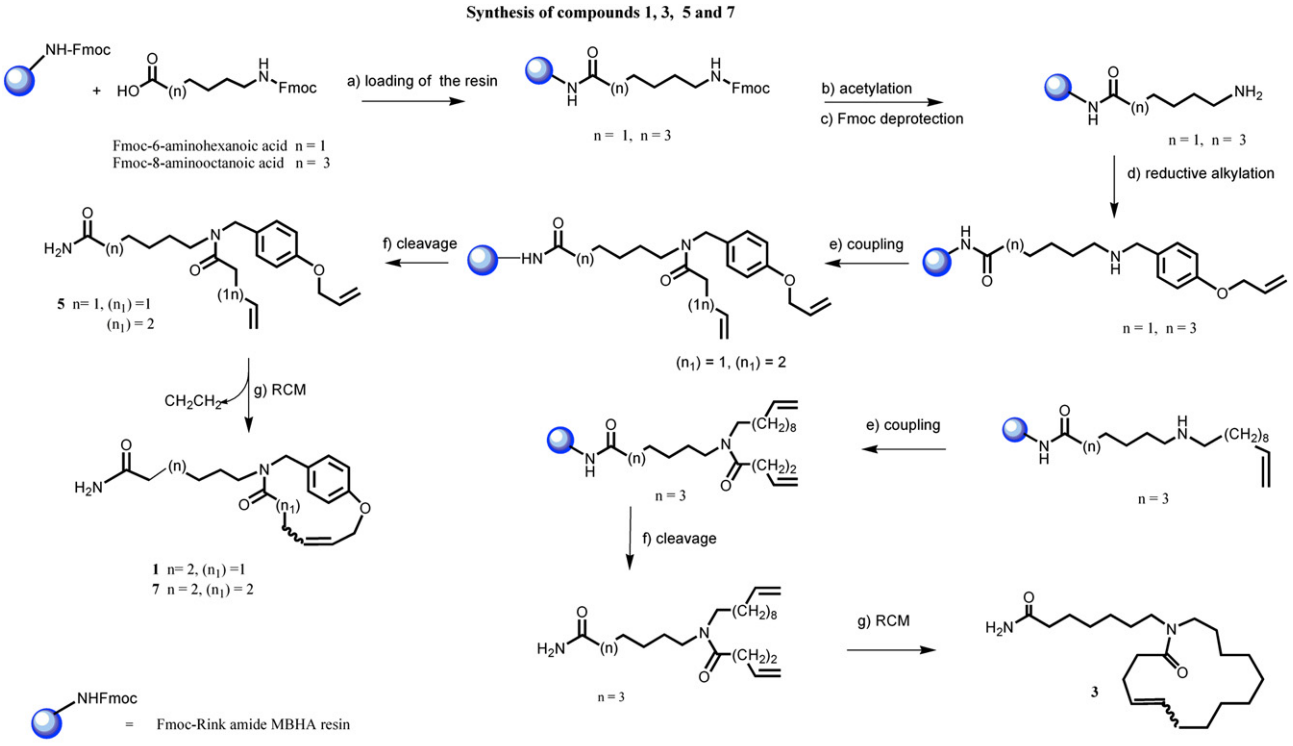

Scheme 2. Synthetic strategy for compounds **1**, **3**, **5**, and **7**.

docking calculations. For all the docking calculations a grid box size of 66×64×48 with spacing of 0.375 Å between the grid points, centered between Zn^{2+} and H170 (x=49.75, y=5.0, z=101.491) and covering the catalytic center surface of HDLP was used. For all the docked structures, all bonds were treated as active torsional bonds except the amide bonds. In order to achieve a representative conformational space during the docking calculations, six calculations consisting of 256 runs were performed, obtaining 1536 structures (256×6). The Lamarckian genetic algorithm was used for dockings. An initial population of 450 randomly placed individuals, a maximum number of 4.0×10^6 energy evaluations, and a maximum number of 3.0×10^6 generations were taken into account. A mutation rate of 0.02 and a crossover rate of 0.8 were used. Results differing by less than 3.5 Å in positional root-mean-square

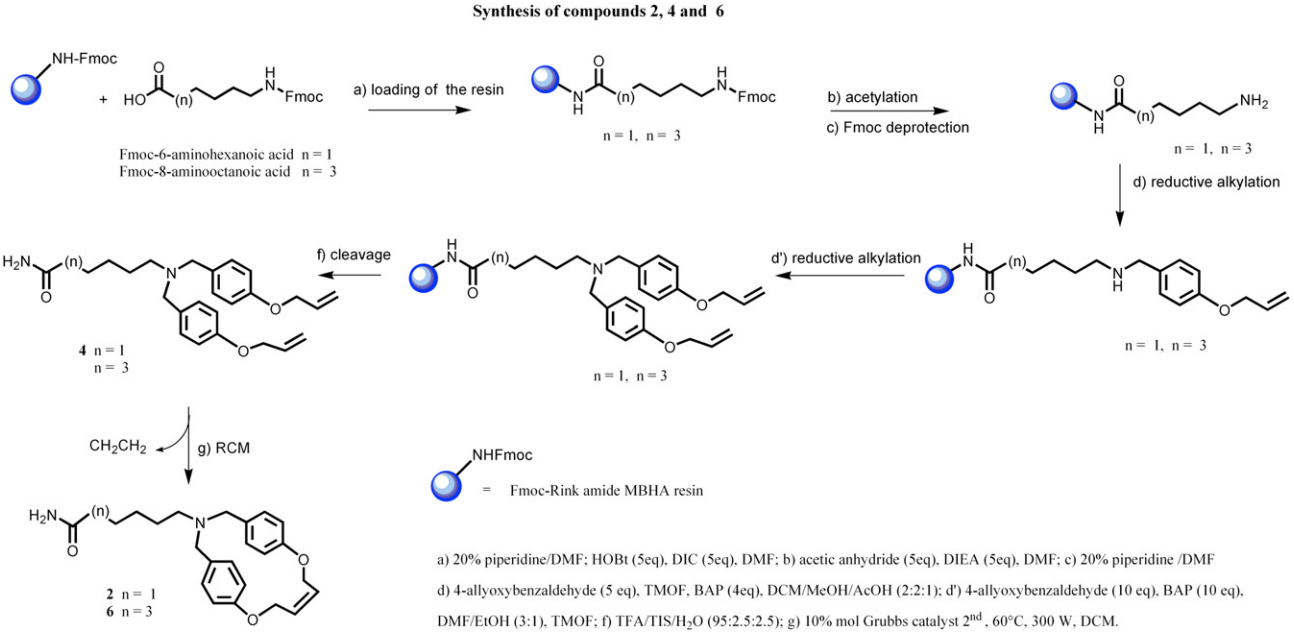

Scheme 3. Synthetic strategy for compounds **2**, **4**, and **6**.

deviation (RMSD) were clustered together and represented by the result with the most favorable free energy of binding. All the 3D models were depicted using the Python software:[27] molecular surfaces are rendered using Maximal Speed Molecular Surface (MSMS).[28]

5.3. General experimental procedures

All the NMR spectra (^{1}H, HMBC, HSQC, TOCSY, COSY, ROESY) were recorded on a Bruker Avance DRX600 at T=298 K. The compounds (**1**–**7**) were dissolved in 0.5 mL of 99.95% DMSO-d_6 (Carlo Erba, 99.95 Atom % D) (^{1}H, δ=2.50 ppm; ^{13}C δ=39.5 ppm) or in 0.5 mL of 99.8% MeOH-d_4 (Aldrich, 99.8+Atom % D). The NMR data were processed on a Silicon Graphic Indigo 2 workstation using UXNMR software. Chemical shifts are expressed in parts per million (ppm) on the delta (δ) scale. Electrospray mass spectrometry (ES-MS) was performed on an LCQ DECA TermoQuest (San Josè, California, USA) mass spectrometer. High resolution mass spectra were acquired on a Q-Tof ULTIMA (Waters, Manchester, UK) calibrated with [Glu]-Fibrinopeptide B fragments using standard experimental conditions.

For estimation of Fmoc amino acids on the resin, absorbance at 301 nm was recorded on a Shimadzu UV 2101 PC. Analytical and semipreparative reverse phase HPLC was performed on a Jupiter C-18 column (250×4.60 mm, 5 μ, 300 Å, flow rate=1 mL/min; 250×10.00 mm, 10 μ, 300 Å, flow rate=4 mL/min, respectively). The binary solvent system (A/B) was as follows: 0.1% TFA in water (A) and 0.1% TFA in acetonitrile (B). The absorbance was detected at 210–240 nm.

All the solvents used for the synthesis were HPLC grade; they were purchased from Aldrich, Fluka, Carlo Erba. Dry dichloromethane was distilled from CaH_2. DCM and DMF used for solid-phase reactions were dried over activated 4 Å molecular sieves. Rink Amide MBHA resin (polymer matrix: copoly(styrene–1% DVB);100–200 mesh, loading level: 0.70 mmol/g and 0.64 mmol/g), HOBt, and HBTU were purchased from Novabiochem. Fmoc-8-Aoc-OH and Fmoc-6-Ahx-OH were obtained from NeoMPS. Trimethyl orthoformate, 4-allyloxybenzaldehyde, undecylenic aldehyde, borane-pyridine complex (BH_3·py, BAP), Grubbs catalyst second generation, 4-pentenoic acid, and 6-eptenoic acid were purchased from Aldrich. Solid-phase syntheses, using the Fmoc strategy, were carried out on a polypropylene ISOLUTE SPE column on a VAC MASTER system, a manual parallel synthesis device purchased from Stepbio. Reactions were generally run under an argon or nitrogen atmosphere. All reagents were purchased from commercial suppliers and used as received.

5.4. Microwave irradiation experiments

All microwave irradiation experiments were carried out in a dedicated CEM-Discover Focused Microwave Synthesis apparatus, operating with continuous irradiation power from 0 to 300 W utilizing the standard absorbance level of 300 W maximum power. The reaction was carried out in 100 mL round-bottomed flask containing a magnetic stirrer and fitted with a reflux condenser.

The Discover™ system also offers controllable ramp time, hold time (reaction time), and uniform stirring. The temperature was monitored using the CEM-Discover built-in-vertically-focused IR temperature sensor. After the irradiation period, the reaction vessel was cooled rapidly (60–120 s) to ambient temperature by air jet cooling.

5.5. General procedures for the synthesis of compounds 1–7

5.5.1. (a) Loading of the resin. The Fmoc-Rink amide MBHA resin (400.0–600.0 mg, loading 0.7 mmol g^{-1}) was placed in a 25 mL polypropylene ISOSOLUTE syringe on a VAC MASTER system, washed with DCM (2×4 mL), DMF (2×4 mL), and swollen in 4 mL of DMF for 1 h. A solution of 20% piperidine in DMF (3 mL, 20 min) was added and then the resin was washed with DMF (3×4 mL).

A solution of Fmoc-8-Aoc-OH or Fmoc-6-Ahx-OH (5 equiv), HOBt (5 equiv), and DIC (5 equiv) in 2.5 mL of dry DMF was added and the mixture was agitated for 3 h under a N_2 stream. The mixture was then removed, the resin was washed with DMF 3×3 mL, DCM 3×3 mL, and dried under vacuum.

5.5.2. (a') Estimation of the level of first residue attachment. The loading of the resin was determined by UV quantification of the Fmoc–piperidine adduct.

The assay was performed on a duplicate samples: 0.4 mL of piperidine and 0.4 mL of DCM were added to two dried samples Fmoc amino acid-resin in two volumetric flasks of 25 mL. The reaction was allowed to proceed for 30 min at room temperature and then 1.6 mL of MeOH was added and the solutions were diluted to 25 mL volume with DCM. A reference solution was prepared in a 25 mL volumetric flask using 0.4 mL of piperidine, 1.6 mL of MeOH, and DCM to volume. The solutions were shaken and the absorbance of the samples versus the reference solution was measured at 301 nm. The substitution level (expressed in mmol of amino acid/g of resin) was calculated from the equation: mmol g^{-1}=(A_{301}/7800)×(25 mL g^{-1} of resin). The obtained loading degree was: 0.34–0.57 mmol g^{-1}.

5.5.3. (b) Acetylation step. DMF (3 mL), DIEA (5 equiv), and acetic anhydride (5 equiv) were combined immediately before use, added to resin, and left to react for 30 min under N_2 stream. After reaction, the resin was washed with DMF 3×3 mL, DCM 3×3 mL, and DMF 3×3 mL(1.5 min each). The reaction was checked using the TNBS test.

5.5.4. (c) Fmoc deprotection. Piperidine (20%) in DMF (3 mL, 1×1.5 min), 20% piperidine in DMF (3 mL, 1×10 min); washings in DMF 2×3 mL, DCM 2×3 mL, and DMF 2×3 mL (1.5 min each).

5.5.5. (d) Reductive alkylation of resin-bound primary amine. The resin was preswollen in DMF, TMOF, and the aldehyde (5 equiv) dissolved in TMOF (2.5 mL) was added. The reaction mixture was shaken at room temperature overnight. The resin was filtered and washed (3×DCM) and dried. The reaction was checked using the TNBS test.

Imine reduction: the resin was suspended in DCM/MeOH/AcOH (2:2:1), BAP (4 equiv) was added, and the mixture was shaken overnight. The resin was filtered and then washed with DMF 2×3 mL, DCM 2×3 mL, MeOH 2×3 mL, DCM 2×3 mL and then dried. HPLC analysis and ESI MS data gave a clear indication of completed reductive amination.

5.5.6. (d') Reductive alkylation of resin-bound secondary amine. The resin was preswollen in DMF, and suspended in TMOF (1 mL). Aldehyde (10 equiv) was dissolved in DMF/EtOH (3:1) (1 mL) and added to the resin, followed by the addition of BAP (10 equiv). The reaction mixture was shaken at room temperature for 4 days, then the resin was filtered and washed with DMF 2×3 mL and DCM 2×3 mL (1.5 min each). HPLC analysis and ESI MS data were used to monitor the reductive alkylation of secondary amine. Quantitative yields were obtained in all the cases.

5.5.7. (e) Peptide coupling conditions. The coupling reaction was promoted by an HOBt/HBTU in DMF coupling protocol.

Carboxylic acid (5 equiv), HOBt (5 equiv), HBTU (5 equiv), and DIEA (10 equiv) were agitated under N_2 in 2.5 mL of DMF for 2 h. After the coupling step, washings were carried out with DMF (3 mL, 3×1.5 min) and DCM (3 mL, 3×1.5 min). The reaction was checked using the HPLC analysis and ESI MS spectra. The yields obtained were >90%.

5.5.8. (f) Cleavage. Cleavage from the resin was performed by a single step treatment with TFA/TIS/H_2O 95:2.5:2.5 for 2 h, under stirring (10 μL×1 mg of resin). Then the resin was filtered off and the beads were washed with neat cleavage mixture (3 mL, 3×1.5 min) and DCM (3×3 mL). The combined filtrates were concentrated in vacuo and lyophilized. Yields were >90% in all cases, with high purity, as determined by HPLC and ESI MS spectra.

5.5.9. (g) RCM under microwave irradiation. Optimized microwave ring closing metathesis.

To a stirred solution (0.3 mM) of the linear precursor in dry DCM was added 10 mol % of Grubbs catalyst second generation. The mixture was refluxed at 60 °C and irradiated at a maximum power (300 W) for 40 min. The reaction mixture was then degassed with N_2 for approximately 1 min to dry off any dissolved ethene, an additional 10 mol % catalyst was added and the solution was stirred and subjected to MW radiation (300 W) for a further 30 min. The mixture was treated with DMSO (50 equiv relative to the catalyst) overnight, finally the solution was concentrated in vacuo and purified by HPLC.

The crude products were purified by semipreparative reverse phase HPLC (on a Jupiter C-18 column: 250×10.00 mm, 10 μ, 300 Å, flow rate=4 mL/min) using the following gradient conditions and characterized by ES-MS and NMR spectra.

5.6. Compound 1

Compound **1** was synthesized following the general procedure *g*. Utilizing 19.1 mg (0.05 mmol) of linear precursor **1e**, 10 mol % of Grubbs catalyst second generation, 0.3 mM solution in dry DCM. The crude reaction was purified by reverse phase semipreparative HPLC.

RP-HPLC t_R=28.20 min from 15% B to 85% B over 60 min; 2.7 mg (15% yield, after HPLC purification step) as a white solid; ES-MS, calcd for $C_{21}H_{30}N_2O_3$ 358.2; found m/z=359.1 $[M+H]^+$. HRMS calcd for $C_{21}H_{31}N_2O_3$ $[M+H]^+$ 359.4819; found 359.4899.

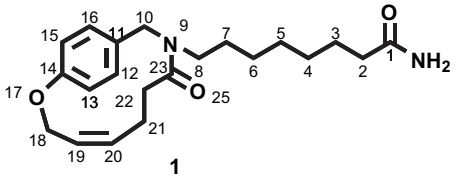

1

^1H and ^{13}C NMR data (600 MHz, MeOH-d_4): δ_H: 1.20–1.70 (10H, m, CH_2-3, CH_2-7), 2.25 (2H, m, CH_2-2), 2.38 (2H, m, CH_2-21), 2.46 (2H, m, CH_2-22), 3.17 (1H, t, J=7.6 Hz, CH-8A), 3.34 (1H, t, J=7.6 Hz, CH-8B), 4.47 (2H, br s, CH_2-10), 4.55 (2H, br s, CH_2-18), 5.57 (1H, br s, CH-19), 5.80 (1H, br s, CH-20), 6.80 (1H, d, J=8.5 Hz, Ar), 6.90 (1H, d, J=8.5 Hz, Ar), 7.07 (1H, d, J=8.0 Hz, Ar), 7.15 (1H, d, J=8.5 Hz, Ar).

δ_C: 24.0 (C-21), 27.2–30.0 (C-3-C-7), 35.0 (C-22), 38.2 (C-2), 50.2 (C-8), 55.1 (C-10), 70.0 (C-18), 111.7 (Ar), 112.0 (Ar), 134.3 (Ar), 135.0 (Ar), 130.0 (C-19-C-20).

5.7. Compound 2

Compound **2** was synthesized following the general procedure *g*. Utilizing 17.0 mg (0.04 mmol) of linear precursor **2e**, 10 mol % of Grubbs catalyst second generation, 0.3 mM solution in dry DCM. The crude reaction was purified by reverse phase semipreparative HPLC.

RP-HPLC t_R=20.6 min from 5% B to 100% B over 60 min; 5.0 mg (32% yield, after HPLC purification step) as a slightly brown oil; ES-MS, calcd for $C_{24}H_{30}N_2O_3$ 394.2; found m/z=395.1 $[M+H]^+$. HRMS calcd for $C_{24}H_{31}N_2O_3$ $[M+H]^+$ 395.2329; found 395.2239.

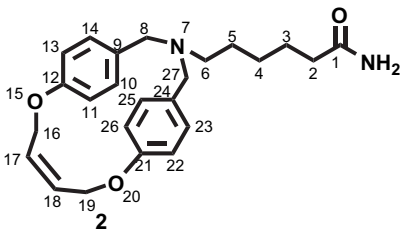

2

^1H and ^{13}C NMR data (600 MHz, DMSO-d_6): δ_H: 1.31–1.38 (4H, m, CH_2-4, CH_2-5), 1.52 (2H, quintet, J=7.6 Hz, CH_2-3), 2.02 (2H, t, J=7.3 Hz, CH_2-2), 3.34 (2H, br s, CH_2-6), 4.13 (2H, d, J=13.3 Hz, CH-16A, CH-19A), 4.66 (2H, d, J=13.3 Hz, CH-16B, CH-19B), 4.75 (4H, br s, CH_2-8, CH_2-27), 5.63 (2H, br s, CH-17, CH-18), 6.47 (2H, d, J=8.5 Hz, Ar), 6.54 (2H, d, J=8.5 Hz, Ar), 6.67 (2H, d, J=8.5 Hz, Ar), 6.94 (2H, d, J=8.5 Hz, Ar), 9.32 (2H, br s, NH_2).

δ_C: 26.3–31.1 (C-3-C-5), 35.3 (C-2), 58.0 (C-6), 62.2 (C-8), 62.2 (C-27), 71.1 (C-19), 72.0 (C-16); 116.4 (Ar), 116.5 (Ar), 129.7 (Ar), 131.1 (Ar), 131.3 (C-17), 131.4 (C-18).

5.8. Compound 3

Compound **3** was synthesized following the general procedure *g*. Utilizing 12.5 mg (0.03 mmol) of linear precursor **3e**, 10 mol % of Grubbs catalyst second generation, 0.3 mM solution in dry DCM. The crude reaction was purified by reverse phase semipreparative HPLC.

RP-HPLC t_R=43.42 min from 15% B to 85% B over 85 min; 2.3 mg (21% yield, after HPLC purification step) as a slightly yellow oil; ES-MS, calcd for $C_{22}H_{40}N_2O_2$ 364.3; found m/z=365.3 $[M+H]^+$. HRMS calcd for $C_{22}H_{41}N_2O_2$ $[M+H]^+$ 365.3163; found 365.2938.

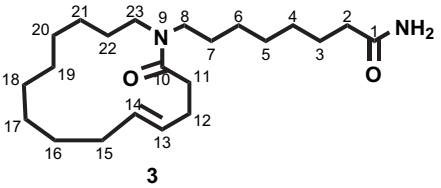

3

^1H and ^{13}C NMR data (600 MHz, DMSO-d_6): δ_H: 1.31–1.58 (10H, m, CH_2-3, CH_2-7), 2.10 (2H, br s, CH_2-2), 2.20 (2H, br s, CH_2-11), 2.32 (2H, br s, CH_2-12), 3.30 (2H, br s, CH_2-8), 1.26–3.31 (18H, m, CH_2-15, CH_2-23), 5.44 (2H, br s, CH-13, CH-14), 9.29 (2H, br s, NH_2).

δ_C: 26.0–31.0 (C-3-C-7), 29.0–35.6 (C-15-C-22), 29.9 (C-12), 30.1 (C-11), 36.0 (C-2), 50.7 (C-23), 52.0 (C-8), 129.0 (C-13-C14).

5.9. Compound 4

Compound **4** was synthesized following the general procedure. A portion of the crude cleaved product (15.0 mg) was then purified as follows: RP-HPLC t_R=25.9 min from 15% B to 85% B over 60 min; 12.5 mg (83% yield, after HPLC purification step) as a yellow oil; ES-MS, calcd for $C_{26}H_{34}N_2O_3$ 422.2; found m/z=423.4 $[M+H]^+$. HRMS calcd for $C_{26}H_{35}N_2O_3$ $[M+H]^+$ 423.2642; found 423.2722.

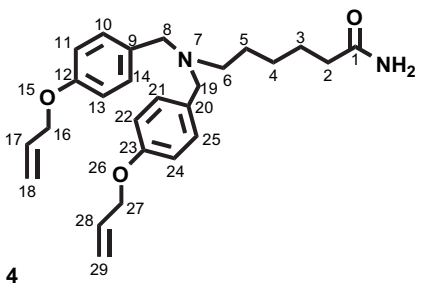

4

^{1}H and ^{13}C NMR data (600 MHz, MeOH-d_4): δ_H: 1.32 (2H, quintet, J=7.5 Hz, CH_2-4), 1.52–1.65 (4H, m, CH_2-3, CH_2-5), 2.14 (2H, t, J=7.2 Hz, CH_2-2), 3.17 (2H, br s, CH_2-6), 4.40 (4H, br s, CH_2-8, CH_2-19), 4.63 (4H, br s, CH_2-16, CH_2-27), 5.29 (2H, br s, CH-18A, CH-29A), 5.42 (1H, br s, CH-18B, CH-29B), 6.05 (2H, m, CH-17, CH-28), 6.72 (2H, d, J=8.5 Hz, Ar), 6.80 (2H, d, J=8.5 Hz, Ar), 7.07 (2H, d, J=8.5 Hz, Ar), 7.15 (2H, d, J=8.5 Hz, Ar).

δ_C: 25.6–31.2 (C-3-C-5), 36.2 (C-2), 52.5 (C-6), 62.2 (C-19), 62.2 (C-8), 70.0 (C-16, C-27), 116.0 (Ar), 116.2 (Ar), 130.0 (Ar), 132.4 (Ar), 112.4 (C-18), 112.6 (C-29), 135.4 (C-28), 135.5 (C-17).

5.10. Compound 5

Compound **5** was synthesized following the general procedure. A portion of the crude cleaved product (20.0 mg) was then purified as follows: RP-HPLC t_R=31.5 min from 15% B to 85% B over 60 min; 13.0 mg (65% yield, after HPLC purification step) as a colorless oil; ES-MS, calcd for $C_{21}H_{30}N_2O_3$ 358.2; found m/z=359.4 $[M+H]^+$. HRMS calcd for $C_{21}H_{31}N_2O_3$ $[M+H]^+$ 359.2329; found 359.2232.

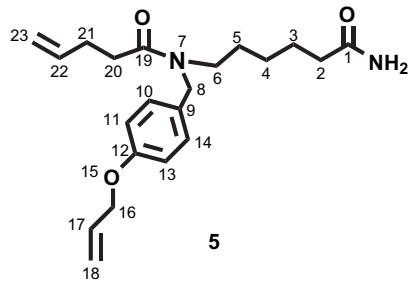

5

^{1}H and ^{13}C NMR data (600 MHz, MeOH-d_4): δ_H: 1.23–1.67 (6H, m, CH_2-3, CH_2-5), 2.16 (2H, t, J=7.2 Hz, CH_2-2), 2.20 (2H, m, CH_2-20), 2.43 (2H, m, CH_2-21), 3.08 (1H, br s, CH-6A), 3.16 (1H, br s, CH-6B), 4.37 (2H, s, CH_2-8), 4.57 (2H, br s, CH_2-16), 5.00 (2H, br s, CH_2-23), 5.30 (1H, br s, CH-18A), 5.45 (1H, br s, CH-18B), 5.75 (2H, m, CH_2-23), 6.02 (1H, m, CH-17), 6.69 (1H, d, J=8.6 Hz, Ar), 6.95 (1H, d, J=9.0 Hz, Ar), 7.09 (1H, d, J=8.6 Hz, Ar), 7.15 (1H, d, J=8.6 Hz, Ar).

δ_C: 27.3–30.0 (C-3-C-5), 30.2 (C-21), 33.0 (C-20), 38.2 (C-2), 50.2 (C-6), 58.4 (C-8), 74.0 (C-16), 113.0 (Ar), 138.0 (Ar), 111.4 (C-18), 113.0 (C-23), 134.4 (C-17), 135.1 (C-22).

5.11. Compound 6

Compound **6** was synthesized following the general procedure *g*. Utilizing 12.5 mg (0.03 mmol) of linear precursor **6e**, 10 mol % of Grubbs catalyst second generation, 0.3 mM solution in dry DCM. The crude reaction was purified by reverse phase semipreparative HPLC.

RP-HPLC t_R=20.20 min from 5% B to 100% B over 65 min; 3.0 mg (22% yield, after HPLC purification step) as a colorless oil; ES-MS, calcd for $C_{26}H_{34}N_2O_3$ 422.2; found m/z=423.4 $[M+H]^+$. HRMS calcd for $C_{26}H_{35}N_2O_3$ $[M+H]^+$ 423.2642; found 423.2339.

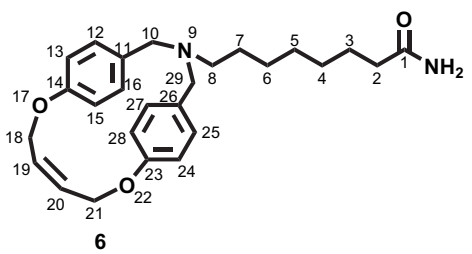

6

^{1}H and ^{13}C NMR data (600 MHz, DMSO-d_6): δ_H: 1.40–1.52 (8H, m, CH_2-4, CH_2-7), 1.67 (2H, m, CH_2-3), 2.24 (2H, t, J=7.2 Hz, CH_2-2), 3.45 (2H, br s, CH_2-8), 4.15 (2H, d, J=13.0 Hz, CH-18A, CH-21A), 4.60 (2H, d, J=13.0 Hz, CH-18B, CH-21B), 4.75 (4H, br s, CH_2-10, CH_2-29), 5.66 (2H, br s, CH-19, CH-20), 6.47 (2H, d, J=8.5 Hz, Ar), 6.54 (2H, d, J=8.5 Hz, Ar), 6.67 (2H, d, J=8.5 Hz, Ar), 6.94 (2H, d, J=8.5 Hz, Ar), 9.32 (2H, br s, NH_2).

δ_C: 25.1–30.1 (C-3-C-7), 35.3 (C-2), 57.9 (C-8), 58.8 (C-29), 58.9 (C-10), 67.8 (C-18, C-21), 116.4 (Ar), 116.45 (Ar), 129.7 (Ar), 131.1 (Ar), 131.4 (C-19, C-20).

5.12. Compound 7

Compound **7** was synthesized following the general procedure *g*. Utilizing 35.5 mg (0.08 mmol) of linear precursor **7e**, 10 mol % of Grubbs catalyst second generation, 0.3 mM solution in dry DCM. The crude reaction was purified by reverse phase semipreparative HPLC.

RP-HPLC t_R=32.30 min from 5% B to 100% B over 65 min; 7.0 mg (21% yield, after HPLC purification step) as a slightly brown solid; ES-MS, calcd for $C_{23}H_{34}N_2O_3$ 386.2; found m/z=387.2 $[M+H]^+$. HRMS calcd for $C_{23}H_{35}N_2O_3$ $[M+H]^+$ 387.2642; found 387.2722.

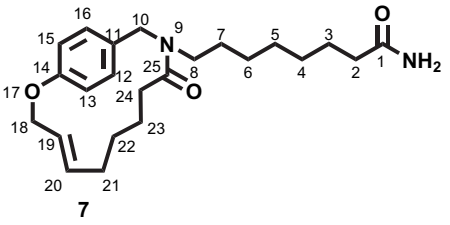

7

^{1}H and ^{13}C NMR data (600 MHz, DMSO-d_6): δ_H: 1.30–1.60 (10H, m, CH_2-3, CH_2-7), 1.34–1.66 (4H, m, CH_2-22, CH_2-23), 2.11 (2H, t, J=7.1 Hz, CH_2-2), 2.05 (2H, m, CH_2-21), 2.25 (2H, br s, CH_2-24), 3.33 (2H, br s, CH_2-8), 4.09 (2H, br s, CH_2-10), 4.59 (2H, br s, CH_2-18), 5.70 (2H, br s, CH-19, CH-20), 6.80 (1H, d, J=8.5 Hz, Ar), 6.89 (1H, d, J=8.5 Hz, Ar), 7.07 (1H, d, J=9.0 Hz, Ar), 7.15 (1H, d, J=8.6 Hz, Ar).

δ_C: 26.1–31.0 (C-3-C-7), 28.8 (C-23), 30.0 (C-22), 30.9 (C-24), 36.0 (C-2), 36.0 (C-21), 52.0 (C-8), 61.8 (C-10), 70.9 (C-18), 114.6 (Ar), 132.4 (Ar), 134.0 (C19-C-20).

5.13. Biological tests

5.13.1. Cells. J774.A1, murine macrophage cell line were grown in adhesion on Petri dishes and maintained with Dulbecco's modified Eagle's medium (DMEM) at 37 °C in DMEM supplemented with 10% fetal born serum (FBS), 25 mM HEPES, 2 mM glutamine, 100 u/mL penicillin, and 100 μg/mL streptomycin. WEHI-164, murine fibrosarcoma cell line were maintained in adhesion on Petri dishes with DMEM supplemented with 10% heat-inactivated FBS, 25 mM HEPES, 100 u/mL penicillin, and 100 μg/mL streptomycin. HEK-293, human epithelial kidney cell line were maintained and grown in adhesion on Petri dishes with DMEM supplemented with 10% FCS, 25 mM HEPES, 100 u/mL penicillin, and 100 μg/mL streptomycin. All reagents for cell culture were from Euroclone (Paignton Devon, UK); [3-(4,5-dimethylthiazol-2-yl)-2,5-phenyl-2*H*-tetrazolium bromide] (MTT) was from Sigma Chemicals (Milan, Italy).

5.13.2. Antiproliferative assay[29]. J774.A1, WEHI-164, and HEK-293 (3.5×10^4 cells) were plated on 96-well plates and allowed to adhere at 37 °C in a 5% CO_2 atmosphere for 2 h. Thereafter, the medium was replaced with fresh medium and serial dilution of each test compound was added and then the cells incubated for 72 h. Cell viability was assessed through an MTT conversion assay. Briefly, 25 μL of MTT (5 mg/mL) was added and the cells were incubated for an additional 3 h. Thereafter, cells were lysed and the dark blue crystals solubilized with 100 μL of a solution containing 50% (v:v) *N*,*N*-dimethylformamide, 20% (w:v) SDS with an adjusted pH of 4.5.[29] The optical density (OD) of each well was measured

with a microplate spectrophotometer (Titertek Multiskan MCC/340) equipped with a 620 nm filter. The viability of each cell line in response to treatment with tested compounds was calculated as: % dead cells=100−(OD treated/OD control)×100. Results were expressed as the concentration of tested compounds able to induce the 50% of mortality in cells (IC_{50}).

Acknowledgements

Financial support by the University of Salerno and by Ministero dell'Istruzione, dell'Università e della Ricerca (MIUR), PRIN-06 are gratefully acknowledged.

Supplementary data

Supplementary data associated with this article can be found in the online version, at doi:10.1016/j.tet.2010.01.061.

References and notes

1. Yoo, C. B.; Jones, P. A. *Nat. Rev. Drug Discov.* **2006**, *5*, 37.
2. Biel, M.; Wascholowski, V.; Giannis, A. *Angew. Chem., Int. Ed.* **2005**, *44*, 3186.
3. (a) Mori, H.; Urano, Y.; Kinoshita, T.; Yoshimura, S.; Takase, S.; Hino, M. *J. Antibiot.* **2003**, *56*, 181; (b) Mori, H.; Abe, F.; Furukawa, S.; Sakai, F.; Hino, M.; Fujii, T. *J. Antibiot.* **2003**, *56*, 80; (c) Mori, H.; Urano, Y.; Abe, F.; Furukawa, S.; Tsurumi, Y.; Sakamoto, K.; Hashimoto, M.; Takase, S.; Hino, M.; Fujii, T. *J. Antibiot.* **2003**, *56*, 72.
4. Rodriquez, M.; Terracciano, S.; Cini, E.; Settembrini, G.; Bruno, I.; Bifulco, G.; Taddei, M.; Gomez-Paloma, L. *Angew. Chem., Int. Ed.* **2006**, *45*, 423.
5. Gomez-Paloma, L.; Bruno, I.; Cini, E.; Khochbin, S.; Rodriquez, M.; Taddei, M.; Terracciano, S.; Sadoul, K. *ChemMedChem* **2007**, *2*, 1511.
6. Finnin, M. S.; Donigian, J. R.; Cohen, A.; Richon, V. M.; Rifkind, R. A.; Marks, P. A.; Breslow, R.; Pavletich, N. P. *Nature* **1999**, *401*, 188.
7. Di Micco, S.; Terracciano, S.; Bruno, I.; Rodriquez, M.; Riccio, R.; Taddei, M.; Bifulco, G. *Bioorg. Med. Chem.* **2008**, *16*, 8635.
8. Nakao, Y.; Yoshida, S.; Matsunaga, S.; Shindoh, N.; Terada, Y.; Nagai, K.; Yamashita, J. K.; Ganesan, A.; van soest, R. W. M.; Fusetani, N. *Angew. Chem., Int. Ed.* **2006**, *45*, 7553.
9. Barrett, A. G. M.; Hennessy, A. J.; Le Vézouët, R.; Procopiou, P. A.; Seale, P. W.; Stefaniak, S.; Upton, R. J.; White, A. J. P.; Williams, D. J. *J. Org. Chem.* **2004**, *69*, 1028.
10. In the calculation, the amine functionality of structures **2**, **4**, and **6** was considered protonated at physiological pH.
11. Halgren, T. A. *J. Comput. Chem.* **1999**, *20*, 720.
12. *MacroModel, Version 8.5*; Schrödinger LLC: New York, NY, 2003.
13. Frisch, M. J.; Trucks, G. W.; Schlegel, H. B.; Scuseria, G. E.; Robb, M. A.; Cheeseman, J. R.; Montgomery, J. A., Jr.; Vreven, T.; Kudin, K. N.; Burant, J. C.; Millam, J. M.; Iyengar, S. S.; Tomasi, J.; Barone, V.; Mennucci, B.; Cossi, M.; Scalmani, G.; Rega, N.; Petersson, G. A.; Nakatsuji, H.; Hada, M.; Ehara, M.; Toyota, K.; Fukuda, R.; Hasegawa, J.; Ishida, M.; Nakajima, T.; Honda, Y.; Kitao, O.; Nakai, H.; Klene, M.; Li, X.; Knox, J. E.; Hratchian, H. P.; Cross, J. B.; Bakken, V.; Adamo, C.; Jaramillo, J.; Gomperts, R.; Stratmann, R. E.; Yazyev, O.; Austin, A. J.; Cammi, R.; Pomelli, C.; Ochterski, J. W.; Ayala, P. Y.; Morokuma, K.; Voth, G. A.; Salvador, P.; Dannenberg, J. J.; Zakrzewski, V. G.; Dapprich, S.; Daniels, A. D.; Strain, M. C.; Farkas, O.; Malick, D. K.; Rabuck, A. D.; Raghavachari, K.; Foresman, J. B.; Ortiz, J. V.; Cui, Q.; Baboul, A. G.; Clifford, S.; Cioslowski, J.; Stefanov, B. B.; Liu, G.; Liashenko, A.; Piskorz, P.; Komaromi, I.; Martin, R. L.; Fox, D. J.; Keith, T.; Al-Laham, M. A.; Peng, C. Y.; Nanayakkara, A.; Challacombe, M.; Gill, P. M. W.; Johnson, B.; Chen, W.; Wong, M. W.; Gonzalez, C.; Pople, J. A. *Gaussian 03, Revision E.01*; Gaussian: Wallingford, CT, 2004.
14. Breneman, C. M.; Wiberg, K. B. *J. Comput. Chem.* **1990**, *11*, 361.
15. Morris, G. M.; Goodsell, D. S.; Halliday, R. S.; Huey, R.; Hart, W. E.; Belew, R. K.; Olson, A. J. *J. Comp. Chem.* **1998**, *19*, 1639.
16. (a) Wang, D.-F.; Wiest, O.; Helquist, P.; Lan-Hargest, H.-Y.; Wiech, N. L. *J. Med. Chem.* **2004**, *47*, 3409; (b) Park, H.; Lee, S. *J. Comput.-Aided Mol. Des.* **2004**, *18*, 375; (c) Wang, D.-F.; Helquist, P.; Wiech, N. L.; Wiest, O. *J. Med. Chem.* **2005**, *48*, 6936; (d) Maulucci, N.; Chini, M. G.; Di Micco, S.; Izzo, I.; Cafaro, E.; Russo, A.; Gallinari, P.; Paolini, C.; Nardi, M. C.; Casapullo, A.; Riccio, R.; Bifulco, G.; De Riccardis, F. *J. Am. Chem. Soc.* **2007**, *129*, 3007; (e) Grolla, A. A.; Podesta, V.; Chini, M. G.; Di Micco, S.; Vallario, A.; Genazzani, A. A.; Canonico, P. L.; Bifulco, G.; Tron, G. C.; Sorba, G.; Pirali, T. *J. Med. Chem.* **2009**, *52*, 7333.
17. The partial charges of the zinc ion, and of the amino acids involved in the catalytic center (A169, H170, D168, D258) have been calculated at DFT B3LYP level and 6-31G(d) basis set using the Chelpg method for population analysis.
18. (a) Aoki, Y.; Kobayashi, S. *J. Comb. Chem.* **1999**, *1*, 371; (b) Abdel-Magid, A. F.; Carson, K. G.; Harris, B. H.; Maryanoff, C. A.; Shah, R. D. *J. Org. Chem.* **1996**, *61*, 3849.
19. (a) Sarantakis, D.; Bicksler, J. *Tetrahedron Lett.* **1997**, *38*, 7325; (b) Swayze, E. E. *Tetrahedron Lett.* **1997**, *38*, 7325; (c) Ayesa, S.; Argrypoulos, D.; Maltseva, T.; Sund, C.; Samuelsson, B. *Eur. J. Org. Chem.* **2004**, 2723.
20. (a) Pande, C. S.; Gupta, N.; Bhardwa, J. *J. Appl. Polym. Sci.* **1995**, *56*, 1127; (b) Bomann, M. D.; Guch, I. C.; Dimare, M. J. *J. Org. Chem.* **1995**, *60*, 5995.
21. Khan, N. M.; Arumugam, V.; Balasubramanian, S. *Tetrahedron Lett.* **1996**, *37*, 4819.
22. (a) Trnka, T. M.; Grubbs, R. H. *Acc. Chem. Res.* **2001**, *34*, 18; (b) Fürstner, A. *Angew. Chem., Int. Ed* **2000**, *39*, 3012.
23. Sol, V.; Chaleix, V.; Granet, R.; Krausz, P. *Tetrahedron* **2008**, *64*, 364.
24. (a) Cornell, W. D.; Cieplak, P.; Bayly, C. I.; Gould, I. R.; Merz, K. M., Jr.; Ferguson, D. M.; Spellmeyer, D. C.; Fox, T.; Caldwell, J. W.; Kollman, P. A. *J. Am. Chem. Soc.* **1995**, *117*, 5179; (b) Weiner, P. K.; Kollman, P. A. *J. Comput. Chem.* **1981**, *2*, 287; (c) Weiner, S. J.; Kollman, P. A.; Case, D. A.; Singh, U. C.; Ghio, C.; Alagona, G.; Profeta, S., Jr.; Weiner, P. K. *J. Am. Chem. Soc.* **1984**, *106*, 765.
25. Still, W. C.; Tempczyk, A.; Hawley, R. C.; Hendrickson, T. *J. Am. Chem. Soc.* **1990**, *112*, 6127.
26. Stote, R. H.; Karplus, M. *Proteins* **1995**, *23*, 12.
27. Sanner, M. F. *J. Mol. Graphics Mod.* **1999**, *17*, 57.
28. Sanner, M. F.; Olson, A. J.; Spehner, J. C. *Biopolymers* **1996**, *38*, 305.
29. Mosmann, T. *J. Immunol. Methods* **1983**, *65*, 55.